Int. J. Heat Mass Transfer. Vol. 12, pp. 915–933. Pergamon Press 1969. Printed in Great Britain

THE MICROLAYER AND BUBBLE GROWTH IN NUCLEATE POOL BOILING

M. G. COOPER

Engineering Department, University of Cambridge, England

(*Received* 5 *July* 1968 *and in revised form* 30 *January* 1969)

Abstract—A theory is presented to determine the rate of growth of a vapour bubble growing from a heated wall in a liquid which is near to saturation temperature. The theory depends on approximate assumptions derived from experiments in which thin liquid layers (microlayers) were observed to occur under such bubbles, and in which the evaporation of the microlayers contributed significantly to the growth of the bubbles. To simplify the analysis it is based on assumptions representative of more extreme situations in which the microlayer predominates, extremes which have not previously been explored. The predictions of the analysis bear some relation (±25 per cent) to the results of experiments with various fluids under conditions for which the assumptions are approximately valid. These predictions, with associated limitations on the ranges of validity of the assumptions, together indicate conditions under which microlayers may be expected to have significant effects on bubble growth. They also have implications for bubble departure size, at standard and reduced gravity. Water, organic liquids, cryogens and metallic fluids are discussed.

The theory is extended to include boiling with liquid bulk temperature differing significantly from saturation temperature.

NOMENCLATURE

B, group defined in equation (8);

C_1, constant in $R = C_1 t^n$;

C_2, constant in $\delta_0 = C_2(\nu_l t_g)^{\frac{1}{2}}$. C_2 is taken to be 0·8;

C_{po}, C_{pv}, C_{pw}, specific heat at constant pressure, for liquid, vapour, wall;

h_{fg}, latent heat of vaporisation;

Ja, Jakob number defined as $\frac{\rho_l}{\rho_v}\frac{C_{pl}(T_{w0} - T_{sat})}{h_{fg}}$;

k_l, k_w, thermal conductivity of liquid, wall;

L_d, L_g, L_s, lengths defined in Appendix A;

n, exponent in $R = C_1 t^n$;

P_d, P_g, P_i, P_s, P_v, pressure terms defined in section 2.1;

Pr_l, Prandtl number for saturated liquid;

r, radial coordinate;

r_c, radius of dried out area;

R, radius of bubble;

R_{di}, R_{is}, R_{ig}, radii defined by equations (21) and (22);

T, temperature. Suffixes: b = bulk, bb = bubble, sat = saturation, w = wall, $w0$ = initial at wall, ∞ = uniform throughout;

t, time coordinate;

t_e, time for microlayer to evaporate to radius considered;

t_g, time for bubble to grow to radius considered;

V_b, volume of bubble;

V_m, volume of vapour evaporated from microlayer;

Greek symbols

α_l, α_w, thermal diffusivity of liquid, wall;

δ, microlayer thickness. Suffix 0 initial value;

μ_l, viscosity of saturated liquid;
ν_l, kinematic viscosity of saturated liquid;
ρ_l, ρ_v, ρ_w, density of saturated liquid, vapour, wall;
σ, surface tension;
ϕ, group defined by equation (10);
ψ, property group defined by equation (11);
θ_T, thickness of thermal boundary layer.

1. INTRODUCTION

THE WORK of many experimenters, summarized in ref. [1] has produced evidence in support of the earlier prediction that, when a liquid boils at a heated wall, a vapour bubble growing at the wall will in some cases leave a thin layer of liquid (the microlayer) on the wall beneath the bubble. An analysis of the hydrodynamics [1], has led to a prediction for the thickness of the microlayer in terms of the time of growth of the bubble, and this prediction lies within ± 25 per cent of the limited observations available. It has also been shown [1] that in some cases evaporation of a microlayer makes a significant contribution to the growth of a bubble. There is a need to "close the loop" in the sense of producing a theory incorporating hydrodynamics and thermodynamics to show the effect of growth rates on microlayer formation and vice versa. For a bubble in a given situation a step-by-step method has been devised [1] to do this, but it is the aim of the present paper to close the loop by simple analytic expressions which indicate whether a microlayer forms and whether it has appreciable effect on the growth of a bubble and heat transfer.

To maintain the desired analytic simplicity while covering the wide range of conditions under which boiling may occur, some approximate assumptions have been made. Of course, if enough assumptions are made, any problem can be "solved". The aim is to make assumptions which are sufficiently accurate over a useful range. It is hoped that this aim has been achieved here by selecting assumptions based on approximations which are valid for the experiments described in ref [1], in which microlayers were observed. They are mainly extreme assumptions, whose validity is confined to the extreme cases in which the microlayer predominates. However, it can be useful to analyse such extremes and this one had not previously been explored. Using results from the extreme case, the analysis is continued to deal with cases in which the microlayer does not predominate.

Experiments reported [1–3] do not conform strictly to the extreme assumptions, but the results bear some relation to the predictions of the analysis, as discussed in section 5 below. From these predictions and the associated limitations on the ranges of validity of the assumptions it has been possible to derive criteria for conditions (broadly, low pressure) under which the microlayer may be expected to have significant effects on bubble growth. They also have implications for bubble departure, at standard and reduced gravity. Water, organic liquids, cryogens and metallic fluids are discussed, but the opportunities to compare theory and observation are limited.

2. BASIS FOR ANALYSIS

The study is primarily concerned with pool boiling with individual bubbles growing effectively in isolation in an otherwise stagnant liquid, reaching sizes greatly in excess of the thickness θ_T of the thermal boundary layer defined as

$$\theta_T = \frac{k_l(T_w - T_b)}{\text{mean heat flux}}.$$

For such bubbles, heat from the thermal boundary layer does not contribute much to bubble growth, for reasons discussed in Appendix A2. Hence the temperature distribution in the thermal boundary layer and the (related) waiting time between bubbles are not considered in the primary argument. Smaller bubbles

growing within the thermal boundary layer are discussed at the end of Appendix A2.

The analysis is initially based on hemispherical bubbles. The shape of bubbles growing near a wall has been observed and discussed by Johnson *et al.* [4] in terms of the relative magnitude of the effects of inertia, viscosity and surface tension. They found that the faster-growing bubbles were nearly hemispherical. Bubbles of other shape are discussed later.

The analysis assumes the formation of a microlayer of thickness in accordance with the hydrodynamic argument and supporting observations reported in [1].

2.1 *Definitions*

If the forces of inertia and viscosity in the vapour are negligible compared with those in the liquid, then the pressure of the vapour in the bubble is nearly uniform. Bubble growth is then determined by the effect of that pressure on the motion of the surrounding liquid. For the purely radial motion arising with a spherical bubble in an infinite mass of liquid with negligible body forces, the "extended Rayleigh equation" applies. It has been used by many writers in the form which states that the pressure in the bubble exceeds the pressure at infinity by

$$\rho(R\ddot{R} + \tfrac{3}{2}\dot{R}^2) + \frac{2\sigma}{R} + 4\mu\frac{\dot{R}}{R}.$$

This can be combined with the equation for conduction of heat in the liquid to deduce the rate of growth of a bubble in an infinite superheated liquid [5].

In [1], Appendix D discusses the application of these terms, respectively called P_i, P_s, P_v to the growth of a bubble near a wall. In addition a term $P_g\,(=(\rho_l - \rho_v)\,gR)$ is introduced there to represent the effect of buoyancy due to gravitational body force. Here in addition it is convenient to consider another term P_d defined by

$$P_d = (T_{w0} - T_{sat})\left(\frac{\mathrm{d}p}{\mathrm{d}T}\right)_{sat}$$

where $(\mathrm{d}p/\mathrm{d}T)_{sat}$ is the slope of the saturation line on the p, T chart at system pressure.

The five terms P_d, P_i, P_s, P_g, P_v cannot readily be linked in any one equation, but their relative sizes indicate the relative importance of the corresponding effects. Comparison of sizes is simple in some cases, particularly for stationary bubbles, in which P_i, P_v are zero, and P_d, P_s, P_g can be evaluated. In discussions of nucleation, the temperature of the bubble T_{bb} is assessed by some means and compared with the saturation temperature at the pressure in the bubble, which is often written as

$$T_{sat} + \frac{2\sigma}{R}\left(\frac{\mathrm{d}T}{\mathrm{d}p}\right)_{sat}$$

Comparing this with T_{bb} is a matter of comparing $2\sigma/R$ (which is P_s) with $(T_{bb} - T_{sat})(\mathrm{d}p/\mathrm{d}T)_{sat}$ (which is some fraction of P_d, depending on the assessment of T_{bb}). Similarly comparison of P_s and P_g indicates whether the bubble will be close to spherical shape or will be greatly affected by gravity. Discussion of the interaction of buoyancy and surface tension forces leading to equilibrium or lift-off can be in terms of P_s and P_g, with other factors arising from bubble shape and contact angle.

For the present problem, the relative sizes of all five terms are significant.

2.2 *Assumptions*

The bubbles of toluene on glass reported in [1] and [6] suggested a set of assumptions which can form the basis for establishing an approximate analysis, leading to a prediction for bubble growth rate. The assumptions used can then be investigated in the light of the analysis.

(1) During most of the growth phase for the toluene bubbles reported in [1], the following inequalities hold:

$$P_d > P_i;\quad P_i > P_s;\quad P_i > P_g;\quad P_i > P_v. \quad (1)$$

For a typical inequality the ratio of the two quantities on opposite sides was in fact of order five, but to provide a basis for simple analysis it

was decided to investigate the effect of assuming that each inequality indicated a ratio of several orders of magnitude. Instead of $P_d > P_i$, etc, it is assumed that $P_d \gg P_i$.

(2) During most of the growth phase for the toluene bubbles, the rate of growth of a bubble is not very different from the rate of evaporation of the microlayer, provided the bulk liquid is nearly at saturation temperature. It was found convenient to express this as:

rate of growth of bubble > rate of evaporation/condensation on the curved surface of bubble

$$\text{or } \frac{dV_b}{dt} > \sum_{\substack{\text{curved}\\ \text{surface}}} \left| \text{evaporation rate} \right| \qquad (2)$$

and again the > sign is tentatively replaced by $\gg$ although again this is not fully justified for the toluene bubble.

(3) During evaporation of the microlayer under the toluene bubbles, the temperature of the glass wall fell by an amount comparable with the initial wall superheat, $T_{w0} - T_{sat}$. However, many other combinations of fluid and wall material will come close to one or other of the two extreme categories: either a poorly conducting liquid on a highly conducting wall, in which case the wall temperature will remain nearly constant during the evaporation period, or at the other extreme a highly conducting liquid, in which case the wall temperature will soon fall nearly to the saturation temperature. These two extremes are much simpler to analyse than the intermediate case represented by toluene on glass. The two extremes are therefore taken as alternative bases for the analysis, namely:

$$\begin{aligned} &\text{(a) } T_{w0} - T_{sat} \gg T_{w0} - T_w \\ &\text{(b) } T_{w0} - T_{sat} \gg T_w - T_{sat}. \end{aligned} \qquad (3)$$

To collect the assumptions together:

$$\left.\begin{aligned} &1.\ P_d \gg P_i; \quad P_i \gg P_s \\ &\qquad\qquad\ \ P_i \gg P_g \\ &\qquad\qquad\ \ P_i \gg P_v \\ &2.\ \frac{dV_b}{dt} \gg \left| \sum_{\substack{\text{curved}\\ \text{surface}}} (\text{evaporation rate}) \right| \\ &3.\ \text{either (a) } T_{w0} - T_{sat} \gg T_{w0} - T_w \\ &\quad \text{or (b) } T_{w0} - T_{sat} \gg T_w - T_{sat}. \end{aligned}\right\} \qquad (4)$$

3. ANALYSIS

For the typical bubble shown in Fig. 1 the rate of growth is assumed to be of the form

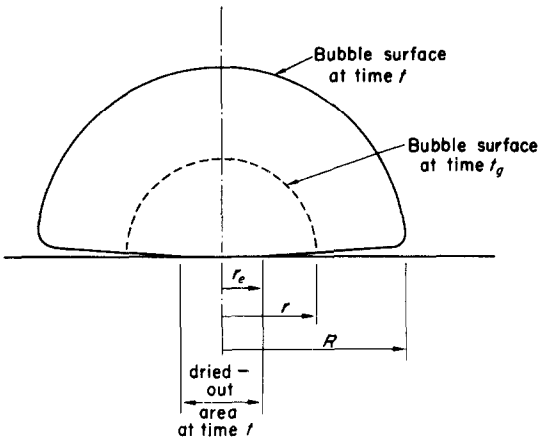

FIG. 1. Hemispherical bubble with microlayer.

$R = C_1 t^n$ as suggested by many experimenters, and the object of this analysis is to determine C_1 and n.

The initial thickness of the microlayer at any point (radius r) is taken from [1] to be $\delta_0 = C_2(v_l t_g)^{\frac{1}{2}}$ where t_g is the time for the bubble to grow to r, i.e. $t_g = (r/C_1)^{1/n}$ and C_2 is a constant, taken to be 0·8.

If at time t the microlayer has completely evaporated within radius r_e then the volume of vapour which has been produced by evaporation of the microlayer up to time t is

$$V_m = \frac{\rho_l}{\rho_v}\left\{\int_0^{r_e} \delta_0 2\pi r\, dr + \int_{r_e}^{R} (\delta_0 - \delta)\, 2\pi r\, dr\right\} \qquad (5)$$

where δ is the remaining thickness of microlayer at the typical point r at time t. This can be

derived from the equation for conduction through the microlayer. Neglecting the thermal capacity of the microlayer, as in ref [1], this equation is:

$$\rho_l h_{fg} \frac{d\delta}{dt} = - k_l \frac{T_w - T_{sat}}{\delta} \quad (6)$$

in which we can take $T_w = T_{w0}$ for a highly conducting wall (assumption 3(a) above). The equation can then be integrated to give

$$\delta_0^2 - \delta^2 = 2 \frac{k_l (T_{w0} - T_{sat})}{\rho_l h_{fg}} (t - t_g) \quad (7)$$

in which $C_2^2 v_l t_g$ can be written for δ_0^2 and then t and t_g can be replaced respectively by $(R/C_1)^{1/n}$ and $(r/C_1)^{1/n}$ to give an expression for δ in terms of r, R and fluid properties. The ratio (r_e/R) can be obtained by setting $\delta = 0$.

Substituting for δ and r_e in equation (5), then integrating and collecting some terms together, we obtain:

$$V_m = \frac{2\pi}{3} R^{(2 + 1/2n)} \frac{B}{C_1^{1/2n}} \quad (8)$$

in which B involves C_2, n, $(T_{wo} - T_{sat})$ and fluid properties, but is independent of R and C_1.

But, by assumption 2 above, this must be the same as the volume of the bubble, which is $\frac{2}{3}\pi R^3$ (a factor $(1 - \rho_v/\rho_l)$ enters here if the microlayer is counted as part of the bubble).

Hence $n = \frac{1}{2}$ and $C_1 = B$, so $R = Bt^{\frac{1}{2}}$.

Evaluating B with $n = \frac{1}{2}$ we obtain

$$R = \frac{2}{C_2} \frac{T_{w0} - T_{sat}}{\phi} (v_l t)^{\frac{1}{2}} \quad (9)$$

where

$$\phi = \psi \left\{ 1 + \frac{2}{C_2^2} \frac{C_{pl}(T_{w0} - T_{sat})}{h_{fg}} \frac{1}{Pr_l} \right\} \quad (10)$$

where

$$\psi = \frac{v_l h_{fg} \rho_v}{k_l} = \frac{\rho_v}{\rho_l} \frac{h_{fg}}{C_{pl}} Pr_l. \quad (11)$$

The quantities ϕ and ψ are each of dimensions of temperature, and ψ is a function of fluid properties alone. For many non-metallic liquids boiling with typical wall superheat, we find

$$1 \gg \frac{2}{C_2^2} \frac{C_{pl}(T_{w0} - T_{sat})}{h_{fg}} \frac{1}{Pr_l}. \quad (12)$$

Hence, taking $\phi \doteqdot \psi$ and writing

$$Ja = \frac{\rho_l}{\rho_v} \frac{C_{pl}(T_{w0} - T_{sat})}{h_{fg}}$$

$$R \doteqdot \frac{2}{C_2} \frac{Ja}{Pr_l} (v_l t)^{\frac{1}{2}} \quad (13)$$

$$\doteqdot 2{\cdot}5 \frac{Ja}{Pr_l} (v_l t)^{\frac{1}{2}} \quad (14)$$

or, in terms of the thermal diffusivity of the liquid, α_l

$$R \doteqdot 2{\cdot}5 \frac{Ja}{Pr_l^{\frac{1}{2}}} (\alpha_l t)^{\frac{1}{2}}. \quad (15)$$

The condition (12) can be shown to imply $r_e \ll R$. Equations (13) to (15) can be obtained by integrating heat flux, taken as $\{k_l(T_{w0} - T_{sat})/\delta\}$ with respect to time and base area with $r_e = 0$ (i.e. neglecting occurrence of dry out) and also regarding δ as constant at its initial value, $C_2(v_l t_g)^{\frac{1}{2}}$. In that integration the two latter approximations are partially counterbalancing, and the condition for validity is not readily assessed.

Using assumption 3(b) above in place of 3(a), the argument proceeds along similar lines, but in place of equation (7) with T_w assumed constant at T_{w0}, we take it instead that heat flow into the microlayer is governed by the equation for heat conduction through the wall, assuming T_w falls rapidly to T_{sat}. Using [7] this gives:

$$\rho_l h_{fg} \frac{d\delta}{dt} = - \frac{k_w (T_{w0} - T_{sat})}{(\pi \alpha_w t)^{\frac{1}{2}}} \quad (16)$$

which leads to

$$R \doteqdot \frac{2}{\pi^{\frac{1}{2}}} \frac{C_{pw}(T_{w0} - T_{sat})}{h_{fg}} \frac{\rho^w}{\rho_v} (\alpha_w t)^{\frac{1}{2}}$$

$$\doteqdot 1{\cdot}12 \left\{ \frac{k_w \rho_w C_{pw}}{k_l \rho_l C_{pl}} \right\}^{\frac{1}{2}} Ja\, (\alpha_l t)^{\frac{1}{2}}. \quad (17)$$

The absence of C_2 from this equation may be surprising, until it is realised that, as with the previous case, we normally have $R \gg r_e$, hence the microlayer does not dry out except over a small central area. Over the remaining area, the heat flow is not affected by δ_0, according to assumption 3(b).

These expressions for bubble growth can be extended as discussed in Appendix A2 to allow for significant evaporation from the curved surface of the bubble as well as the microlayer.

4. COMPARISON WITH SPHERICAL BUBBLE IN INFINITE LIQUID

The discussion so far has predicted the rate at which a hemispherical bubble will grow in a saturated liquid, due solely to evaporation of a microlayer from a wall, assumed highly conducting in the first instance (assumption 3(a)). It is of interest to compare this with the rate of growth predicted by Scriven [5] for a bubble growing with spherical symmetry in an infinite liquid initially at uniform temperature T_∞ ($> T_{sat}$). In principle the two cases are very different, but nevertheless the latter has been applied in the past to some cases of bubbles growing at a wall, where it may now be felt that a microlayer would be present.

For non-metallic fluids in our range of interest, Scriven [5] arrives at the expression:-

$$R = 2\left(\frac{3}{\pi}\right)^{\frac{1}{2}} \frac{(T_\infty - T_{sat})(\rho_l C_{pl} k_l t)^{\frac{1}{2}}}{\rho_v\{h_{fg} + (C_{pl} - C_{pv})(T_\infty - T_{sat})\}} \tag{18}$$

$$= \left\{\frac{C_2(3/\pi)^{\frac{1}{2}} Pr_l^{\frac{1}{2}}}{1 + (C_{pl} - C_{pv})(T_\infty - T_{sat})/h_{fg}}\right\} \times \left\{\frac{2}{C_2}\frac{C_{pl}(T_\infty - T_{sat})}{h_{fg}}\frac{\rho_l}{\rho_v} Pr_l^{-\frac{1}{2}}(\alpha_l t)^{\frac{1}{2}}\right\}. \tag{19}$$

For many non-metallic fluids at normal wall superheats the first bracket lies between 0·5 and 2·0. The second bracket differs from the expressions for R in equations (13)–(15) only in having T_∞ in place of T_{w0}.

Hence if Scriven's expression equation (18) above for growth of spherical bubbles in an infinite fluid initially at temperature T_∞ is applied to a hemispherical bubble growing in a fluid initially at T_{sat} on a highly conducting wall at T_{w0}, then for many non-metallic liquids, provided T_{w0} is written for T_∞ the answer so obtained is roughly similar to that obtained by microlayer arguments in this paper, equation (14), although the mechanism and theory are quite different.

5. COMPARISON WITH EXPERIMENTAL RESULTS

Many experimenters have reported observations of bubble growth rates. Of those known to the author, a limited number from [1–3, 6] are applicable, in the sense that the inequalities of equation (1) hold (as single inequalities $>$ not $\gg$) during most of the growth phase.

It is to be expected that the toluene bubbles of [1] and [6] are applicable, since the inequalities were based on them. However, there is the difficulty that the wall temperature is neither nearly constant at T_{w0} as required for inequality 3(a) nor nearly constant at T_{sat} as required for inequality 3(b). Assumption 3(a) is adopted, using for T_{w0} a mean value of T_w based on averaging the observed value of $(T_w - T_{sat})$ throughout the growth period and across the base area of the bubble. The prediction of equation (14) is then within ± 25 per cent of the observed growth of the bubble.

Some bubbles reported in [3] are applicable, provided again the wall temperature can be assessed. The wall in these experiments was a thin strip of zirconium, 0·25 mm thick. For organic liquids, zirconium acts as a highly conducting wall, so assumption 3(a) applies, but the finite thickness will affect heat flow after a time of the order of $(\text{thickness})^2/\alpha_w$ which is approximately 5 ms. Hence the wall temperature is taken to be constant at its reported value, for growth periods of up to 5 ms.

For all applicable bubbles from [1], [3] and [6] bubble growth is well represented by $R \propto t^{\frac{1}{2}}$. Experiment and theory are therefore conveniently compared in Fig. 2, which shows the

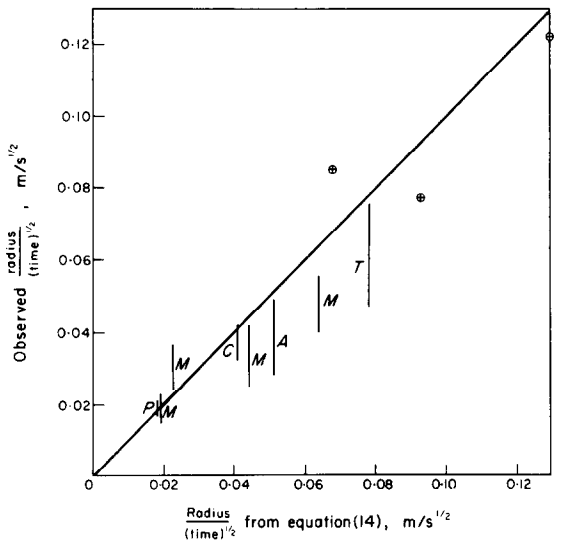

FIG. 2. Comparison of observed and predicted values of (radius)/(time)$^{\frac{1}{2}}$ ⊕—toluene [6]; *A*—acetone [3]; *C*—carbon tetrachloride [3]; *M*—methanol [3]; *P*—*n*-pentane [3]; *T*—toluene [3].

observed value of (radius)/(time)$^{\frac{1}{2}}$ in m/s$^{\frac{1}{2}}$ for the parabola of best fit during the growth phase, plotted linearly as ordinate against the theoretical value of (radius)/(time)$^{\frac{1}{2}}$ derived from equation (14). Where several bubbles are reported under nominally identical conditions, Fig. 2 shows the range of values of $R/t^{\frac{1}{2}}$ observed. These graphs could have been presented in dimensionless form by dividing by either $v_l^{\frac{1}{2}}$ or $\alpha_l^{\frac{1}{2}}$ but there seems no clear reason for choosing one or the other.

The points in Fig. 2 derived from [6] lie close to the 45° line. The points from [3] lie typically some 25 per cent below that line. However, in [3] the authors give an equivalent bubble diameter, determined by a method (discussed in appendix B below), which suits their aims, but would lead to an underestimate of radius if the bubble were hemispherical. The extent of the underestimate depends on the shape of the bubble, and that changes during growth, but in early stages it is likely to be of the order of 30 or 60 per cent. Increasing their results by 45 per cent would bring them closer to the 45° line, then in most cases the 45° line would lie within the scatter among results in [3] under nominally identical conditions. Exceptions to this occur with the slower growing bubbles, possibly because they were also small, and the thermal boundary layer might have an effect, as discussed in Appendix A2.

In view of the extreme assumptions and the difficulty in determining T_w, this agreement is regarded as satisfactory, at least for the main purpose of the present work, which is to provide a basis for assessing circumstances in which the microlayer is or is not important. The assessment proceeds partly by re-consideration of the underlying assumptions, and introducing further comparison with experiment, for bubbles classed as inapplicable above.

6. RE-CONSIDERATION OF ASSUMPTIONS

6.1. *Analysis*

The assumptions 1–3 of equation (4) can now be re-cast in more convenient form. Details of the algebra are given in appendixes A1–A3 respectively, but results can be summarised as follows:

(1) For assumptions 1 expressions for $\dot{R}$, $\ddot{R}$ can be derived from equation (9), expressed in terms of R by use of equation (9) and substituted into P_i etc.

(2) For assumption 2 an expression is developed in Appendix A2 for the growth of a bubble due to the two mechanisms of evaporation of microlayer and evaporation at the curved surface provided the bubble radius is much greater than θ_T. From this a condition is deduced that the former mechanism predominates.

(3) For assumptions 3(a) and (b) expressions for the fall in T_w can be compared with $(T_{w0} - T_{sat})$.

If assumption 3(a) is adopted, the complete set of assumptions can be expressed in terms of $(T_{w0} - T_{sat})$ as follows:

$$\left.\begin{array}{lll} 1. & \left\{\frac{C_2}{2}\right\}^{\frac{1}{3}}\left\{\frac{R}{L_d}\right\}^{\frac{2}{3}} \gg \frac{T_{w0}-T_{sat}}{C_2\phi}; & \frac{T_{w0}-T_{sat}}{C_2\phi} \gg \left\{\frac{R}{L_s}\right\}^{\frac{1}{4}} \\ & & \frac{T_{w0}-T_{sat}}{C_2\phi} \gg \left\{\frac{R}{L_g}\right\}^{\frac{2}{3}} \\ & & \frac{T_{w0}-T_{sat}}{C_2\phi} \gg 2 \\ 2. & & T_{w0}-T_{sat} \gg C_2(3/\pi)^{\frac{1}{2}}\, Pr_l^{\frac{1}{2}}\,|T_{sat}-T_b| \\ 3(a) & & T_{w0}-T_{sat} \gg 3\frac{h_{fg}}{C_{pl}}\frac{k_l\rho_l C_{pl}}{k_w\rho_w C_{pw}} \end{array}\right\} \quad (20)$$

where the characteristic lengths L_d, L_s, L_g involve only the properties of the fluid and the local gravitational acceleration g, as defined in Appendix A. As noted earlier, $(T_{w0} - T_{sat})/\phi \doteqdot Ja/Pr$.

Corresponding expressions which apply when assumption 3(b) is used in place of 3(a) can be derived similarly.

In this form the assumptions can be shown graphically as defining regions on a chart of system pressure against initial wall superheat $(T_{w0} - T_{sat})$ for any given bubble radius R and any fluid—wall combination and bulk temperature. This is done in Fig. 3 for $R = 1$ mm for water boiling on copper at bulk subcooling 1·3 degC. The conditions are all met in the cross-hatched region. In the shaded region above and to the left of this, the condition $P_d \gg P_i$ fails. Below and to the right of the region, the conditions

$$P_i \gg P_s$$
$$P_i \gg P_g$$

fail. Further below the other conditions fail.

For different values of R the regions lie in different positions. The positions are easily established, but the figure becomes complicated, making this an inconvenient method of visualising the problem. Instead it is more convenient to re-cast again the conditions principally involved, namely:

$$P_d \gg P_i; \quad \begin{array}{l} P_i \gg P_s \\ P_i \gg P_g \end{array}$$

in the form:

$$L_d\left\{\frac{C_2}{2}\right\}^{\frac{1}{2}}\left\{\frac{T_{w0}-T_{sat}}{C_2\phi}\right\}^{\frac{3}{2}} \ll R; \quad \left.\begin{array}{l} R \ll L_s\left\{\frac{T_{w0}-T_{sat}}{C_2\phi}\right\}^4 \\ R \ll L_g\left\{\frac{T_{w0}-T_{sat}}{C_2\phi}\right\}^{\frac{4}{3}} \end{array}\right\} \quad (21)$$

or

$$R_{di} \ll R; \quad \begin{array}{l} R \ll R_{is} \\ R \ll R_{ig} \end{array} \quad (22)$$

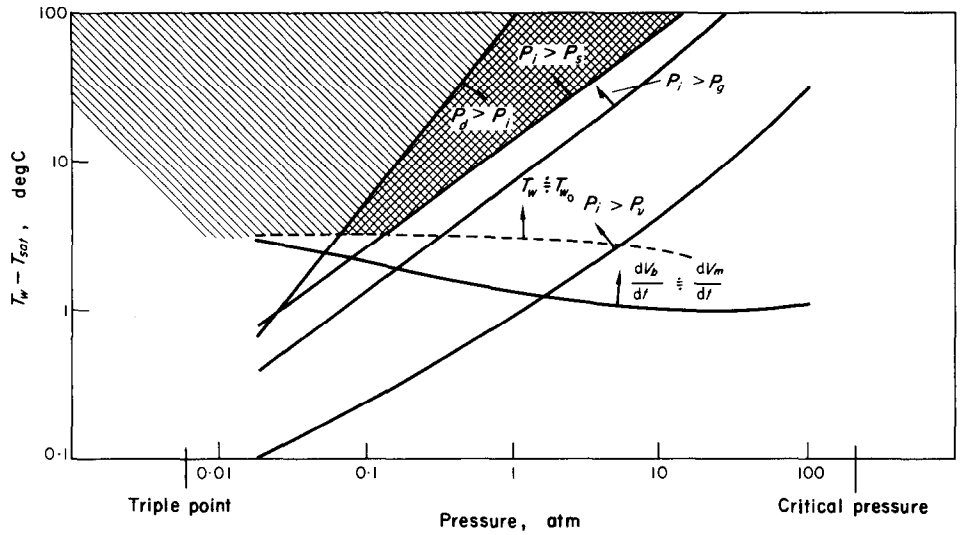

FIG. 3. Graphical representation of equation (20) for water boiling on copper, with bulk subcooling less than 1·3 degC. All inequalities hold (> not ≫) inside cross-hatched area, with $R = 1$ mm.

which can readily be applied to any specified fluid and operating pressure and wall temperature.

6.2 *Consideration of inequalities in terms of* R_{di}, R_{is}, R_{ig}

The inequality $R_{di} \ll R$ is equivalent to $P_d \gg P_i$

$$\text{or} \quad (T_{w0} - T_{sat}) \left(\frac{dp}{dT}\right)_{sat} \gg \rho_l(R\ddot{R} + \tfrac{3}{2}\dot{R}^2)$$

$$\text{or} \quad (T_{w0} - T_{sat}) \gg \rho_l(R\ddot{R} + \tfrac{3}{2}\dot{R}^2)\left(\frac{dT}{dp}\right)_{sat}$$

implying that the change in saturation temperature due to inertia stresses is much less than the wall superheat. This is necessary if the temperature at the top of the microlayer (T_{int}) is to be put equal to T_{sat}. If the inequality fails, then the temperature of saturated vapour at the pressure in the bubble is appreciably greater than T_{sat}, so T_{int} is appreciably greater than T_{sat}, so conduction of heat through the microlayer is reduced and bubble growth is slowed.

The inequality inevitably fails when the bubble is very small, but for many cases (including those reported in Fig. 2) R_{di} is small compared with the maximum radius of the bubble, so the inequality holds (> if not ≫) during most of the time the bubble is growing. The effect of early failure appears to be slight, possibly because R_{di} is of order θ_T hence the early reduction in growth rate is partly counterbalanced by evaporation due to the superheat in the thermal boundary layer, as discussed in Appendix A2.

For some cases reported in [3] R_{di} is several mm, which is an appreciable fraction of the maximum radius of the bubble and well in excess of θ_T. For those cases the present theory implies that bubble growth is slowed for an appreciable part of the growth period. Nevertheless, it still seems that a microlayer will form, although the equations governing its evaporation will be different. A partial analysis is given in Appendix B, and that predicts a linear growth, with $R \propto t$. A few experimental observations are available, permitting comparison subject to reservations discussed in Appendix B. As shown there, the comparison is promising.

The inequality $R \ll R_{is}$ *is equivalent to* $P_i \gg P_s$, implying that inertia stresses greatly exceed the stress due to surface tension ($2\sigma/R$). The inequality fails in due course as a bubble grows, then surface tension stresses predominate over inertia stresses and the bubble tends to round off towards spherical shape, from its original hemispherical shape. It may seem strange that surface tension should emerge as the predominant force when the bubble grows, since P_s is in fact falling (as R^{-1}). However, P_i is falling faster (as R^{-2}) so P_s eventually predominates. Matters are complex, but from photographs in [2] and [3] it appears that even when the radius is well in excess of R_{is} the bubble still has an appreciable area of flat base in contact with the wall. Nevertheless, the rate of growth of that base radius is much below the rate implied by the theory above, hence the microlayer is presumably thicker and of smaller plan area. Both of these changes will reduce the contribution of the microlayer to bubble growth beyond R_{is}.

This case is illustrated by one set of bubbles from [2] and two from [3], for each of which R_{is} lies between 0·3 and 0·4 mm. The observed growth curves are reproduced as Figs. 4(a), (b), (c), on each of which the prediction of equation (14) is also shown. The first few frames of each cine film are very significant, and as far as can be judged from them, the growth in Figs. 4(a) and (b) is initially in accordance with equation (14), up to a radius a few times R_{is}, after which there is a marked change to a slower growth, bearing

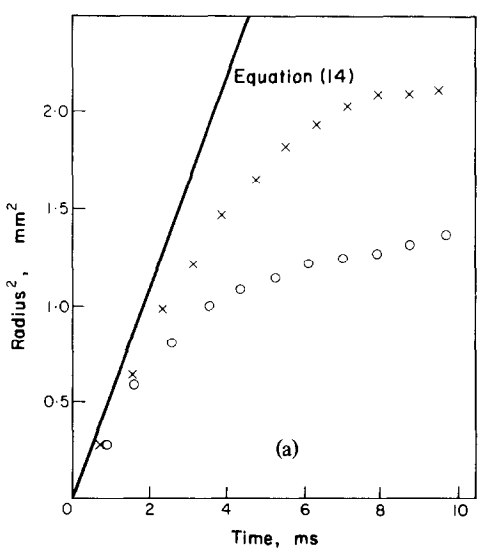

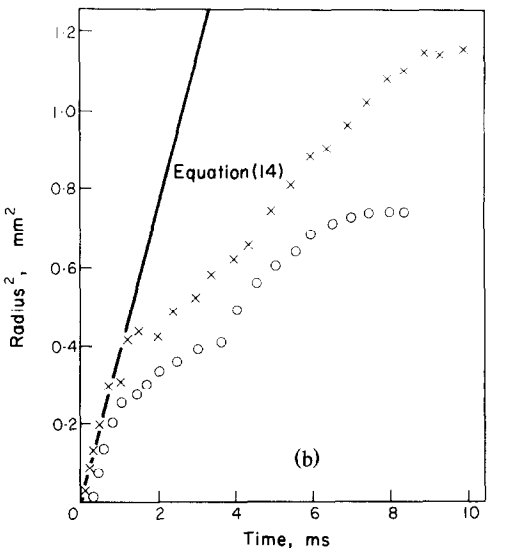

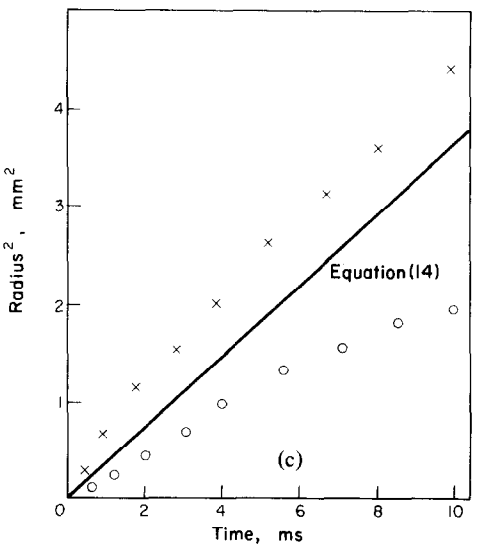

FIG. 4. Observed growth rates compared with equation (14) for bubbles having R_{is} 0·3 mm to 0·4 mm. (a) Water at 1 atm [2], (b) *n*-pentane at 0·69 atm [3]; (c) methanol at 0·52 atm [3]. Scatter among nominally identical tests is indicated by × (maximum) ○ (minimum).

no relation to equation (14). In Fig. 4(c) growth is in accordance with equation (14) for a much longer time, suggesting that some other factor may be significant.

The rounding off which follows when R exceeds R_{is} may also lead to a tendency for the bubble to lift off the wall, a tendency which is absent if the bubble remains hemispherical. (section 5·5 of [1]). This tendency will be opposed by the action of thermocapillarity, according to [8]. Consideration of R_{is} may therefore provide a criterion for bubble departure, even in the absence of gravitational effects, and this is discussed below (section 6.3).

In some cases (broadly, at high pressure) R_{is} is very small, of the order of 10^{-6} m. At such small sizes the bubble is usually deep in a thermal boundary layer. Its growth is thus much influenced by superheat in the surrounding liquid causing evaporation at the curved surface in addition to evaporation of the microlayer. The matter is discussed in Appendix A2, where it is shown that, while $R < \theta_T$, growth rate is substantially faster than that used to establish equation (22). Since $R_{is} \propto$ (growth rate)^4 this suggests that a bubble deep in the thermal boundary layer will not round off until R greatly exceeds R_{is} as determined from equation (22). However, after the bubble has grown well through the thermal boundary layer and evaporation from the curved surface has fallen off, then microlayer evaporation is not fast enough to prevent the bubble from rounding off. Hence the growth and final size of such bubbles will be determined more by the thickness of the thermal boundary layer.

The way in which bubbles round off during growth has been reported and discussed by earlier experimenters, often in terms of variation of the apparent contact angle at the apparent triple interface where the outer edge of the bubble appears to meet the wall. If a microlayer is present, this is not a true triple interface, but an apparent "corner" on the bubble at the outer edge of the microlayer. However, some equations which have been used, such as force balances based on surface tension and contact angle, can still be applied, provided it is recognised that the force is not acting directly on the wall but is instead transmitted to the wall by local variation of fluid stress near the "corner".

The inequality $R \ll R_{ig}$ is equivalent to $P_i \gg P_g$ implying that inertia stresses greatly exceed the hydrostatic head due to one bubble radius ($\rho g R$). The inequality fails in due course as a bubble grows, and buoyancy forces then become significant compared with inertia stresses, so there is a tendency for the bubble to move off. Nevertheless, to judge from data in [3], that failure does not cause any immediate change in growth pattern. Instead the radius continues to grow in accordance with equation (14) until it is several times R_{ig}.

6.3 *Bubble departure*

Consideration of R_{is}, R_{ig} in section 6.2 above suggests that as the radius grows beyond either of these values there is an increasing tendency for the bubble to depart. If the smaller of R_{is}, R_{ig} is less than the thickness θ_T of the thermal boundary layer, then as discussed in 6.2 above and in Appendix A2, the theory leading to R_{is}, R_{ig} fails, and must be replaced by one allowing for the thermal boundary layer. In that, θ_T is likely to emerge as the stronger influence on bubble growth and final size.

Many experimenters have reported on the boiling of water, giving the sizes of the bubbles of steam as they leave the heater surface. Summaries have been prepared by Cole [9] and by Cole and Shulman [10], plotting departure size against, for example, system pressure irrespective of other conditions such as wall superheat. Such graphs show a trend, broadly (pressure)$^{-n}$ with $n = 0{\cdot}6$ or $1{\cdot}0$ and a wide scatter band. The values of R_{is} and R_{ig} from Table 1 (whichever is the smaller) for pressures of 0·1 and 1·0 atm and wall superheat 10°C are consistent with the trend and within the scatter band, but at pressures above 1 atm the observed bubble sizes greatly exceed the smaller of R_{is}, R_{ig} suggesting again that other

Table 1. Values of R_{di}, R_{is}, R_{ig} for saturated boiling, equation (22)

Fluid	Pressure (atm)	$T_{w0} - T_{sat}$ (degC)	R_{di} (mm)	R_{is} (mm)	R_{ig} (mm)
Toluene	0·1	20	0·70	80·4	7·9
Water	0·1	10	2·5	229	15
Water	1·0	10	0·03	0·30	1·55
Water	10·0	10	0·0003	0·003	0·11
Oxygen	0·0015	5	25·9	10^4	36·4
Oxygen	1·0	5	0·0012	0·003	0·19
Nitrogen	0·124	5	0·042	0·85	1·34
Nitrogen	1·0	5	0·0008	0·002	0·17
Helium	0·05	5	0·073	474	5·84
Helium	1·0	5	0·0003	0·18	0·32
Hydrogen	0·07	5	0·061	10·19	3·72
Hydrogen	1·0	5	0·0002	0·002	0·23
Acetone	0·29	27·2	0·13	14·1	4·4
Carbon tetrachloride	0·18	28·9	0·15	10·5	3·26
n-Pentane	1·0	17·2	0·003	0·02	0·46
n-Pentane	0·71	27·7	0·012	0·39	1·2
Methanol	0·523	20·0	0·016	0·31	1·19
Methanol	0·40	20·0	0·029	0·75	1·61
Methanol	0·27	26·7	0·10	8·18	3·58

mechanisms are involved, possibly involving θ_T or thermocapillarity. The dynamics of bubble growth and departure are complex, and the main contribution of the present paper to this problem is to suggest that at low pressures the microlayer may be one of the factors. Further study involving reduced gravity may help to clarify problems of bubble dynamics and the microlayer. Conversely, consideration of R_{is} and R_{ig} may throw light on the reported experiments showing that heat flux in nucleate boiling is nearly independent of gravity in some cases, [11, 12]. Where low pressure is combined with low gravity, as in some space applications, R_{is} and R_{ig} may both be very large, so an understanding of the microlayer may be very important.

7. SUMMARY AND APPLICATION TO PARTICULAR FLUIDS

7.1 *Non-metallic fluids*

For saturation boiling from a highly conducting wall, the range of applicability of the present theory is indicated by the values of R_{di}, R_{is}, R_{ig} and these are tabulated in Table 1 for some fluids and conditions of interest. All fluids differ in detail, and wall superheat is an important factor, but it can be seen that the required conditions (broadly $R_{di} < 0{\cdot}3$ mm, and R_{ig}, R_{is} each > 5 mm) are generally obtained with the non-metallic fluids listed when the pressure is between 0·1 and 0·5 atm. Because many industrial applications involve boiling of water at pressures well above 1 atm, Table 1 includes values for water at 10 atm. The value of R_{is} is then very small (3×10^{-6} m) and this suggests that, as discussed in section 6.2, the bubble will tend to round off at small size, a few times θ_T. Hence for water at more than about 1 atm, the thermal boundary layer has greater effect on bubble growth than microlayer phenomena. Table 1 also shows data for boiling of cryogens at atmospheric pressure and 5°C wall superheat, when R_{is} is generally small, indicating again that the bubbles will tend to round off at small sizes. Data are also included for boiling of cryogens near the triple points (precise properties at the triple points could not be located in all cases). Where triple point pressure is well below 1 atm, it seems that

microlayer phenomena can be significant. For nitrogen the triple point is at about 1/8 atm, so boiling cannot be strongly dependent on microlayer phenomena. For carbon dioxide the triple point is at 5·1 atm, and microlayer phenomena cannot become significant.

For subcooled boiling from a highly conducting wall, the effect of conduction to the bulk liquid will complicate the picture, though it can still be analysed as discussed in Appendix A2. It is shown there that such conduction has little effect if expression 2 of equation (20) holds. When this is evaluated for the same fluids, with $Pr_l \approx 6$, it requires

$$|T_{sat} - T_b| \ll 0{\cdot}5\,(T_{w0} - T_{sat})$$

so bulk subcooling is to be well below wall superheat. This is often met, and the earlier paragraph then applies.

For saturation boiling from a moderately conducting wall, the effect of falling wall temperature will complicate the picture, depending on the ratio of the values of the product $(k\rho C_p)$ for liquid and wall, as shown by expression 3 of equation (20). Water has a comparatively high value of $(k\rho C_p)$, so the complication arises unless the wall is a very good conductor like copper, hence Fig. 3 was calculated for copper. For the other non-metallic fluids discussed, $(k\rho C_p)$ is lower by a factor 6 or more, so other metals such as mild steel are sufficiently highly conducting for the simple theory to apply. At the other extreme, with water boiling on glass, the analysis should be based on assumption 3(b) and equation (17).

The present theory is thus relevant to many boiling situations at sub-atmospheric pressure. Some de-salination plants involve boiling at such pressures, but usually from a flowing stream not from a heated wall. Some situations of cryogens boiling in space vehicles may be applicable.

7.2 *Metallic liquids*

In studying boiling of metallic liquids such as sodium there are obvious experimental difficulties, and no data seem to be available on bubble growth or surface temperature. However, the hydrodynamic arguments of [1] leading to initial microlayer thickness $\delta_0 = C_2(\nu_l t_g)^{\frac{1}{2}}$ should still be applicable, if the manner of growth of the bubbles were known. In the thermodynamic arguments of the present paper, assumption 3(b) must be substituted for 3(a), leading to equation (17). The form of assumption 2 then differs from that in equation (20) and will seldom be met, as it places a close restriction on the subcooling or superheating permitted in the liquid around the bubble. Such a restriction is particularly unrealistic in view of the thick thermal boundary layers encountered with sodium. These difficulties reflect the fact that, although a microlayer may form, it will not be so important for heat transfer with sodium as it is for the cases considered earlier which involved less conducting liquids on fairly well conducting walls. For those cases, any microlayer constituted an area where heat was transferred rapidly from the wall, at a rate often greatly exceeding that for transfer across the curved surface of the bubble. For the sodium, by contrast, the heat flow across the curved surface of the bubble will be of the same order as that through the microlayer, assuming the sodium and wall both have similar conductivity and initial superheat. The microlayer is therefore unlikely to cause more than a fractional increase in heat flow.

8. CONCLUSIONS

For many non-metallic fluids boiling from a heated wall at pressures well below 1 atmosphere, the assumptions listed in equation (4) will be valid during much of the growth period. In that case a microlayer can be expected to form and virtually dominate later stages of growth of bubbles, when the radius greatly exceeds θ_T and growth continues in accordance with:

$$R = \frac{2}{C_2}\frac{T_{w0} - T_{sat}}{\phi}(\nu_l t)^{\frac{1}{2}} \doteq 2{\cdot}5\frac{Ja}{Pr_l}(\nu_l t)^{\frac{1}{2}}. \quad (14)$$

Limitations to the validity of the assumptions are summarized in Table 1 and equation (22). For boiling at higher pressures the microlayer may still occur, making contributions to bubble growth and heat transfer, but the microlayer will not on its own cause the bubble radius to grow much beyond θ_T.

The expressions derived by Scriven [5] for bubble growth in an infinite liquid initially at uniform temperature T_∞ gives answers numerically similar to the above expression if T_∞ is put equal to T_{w0}. The physical situations, theory and analysis are all very different, but this numerical similarity is noteworthy because expressions such as Scriven's have been used by others with moderate success in theories predicting bubble growth without allowing for the microlayer although it now seems that microlayers were present in some cases.

A bubble growing at a wall in a liquid which is not at saturation temperature will be affected by microlayer evaporation and evaporation (condensation) at the curved surface. The net growth is predicted by adding the radial growth (collapse) rates appropriate to the two separate mechanisms.

The contribution of the microlayer to the growth pattern may affect departure of the bubble, because

(1) As the bubble grows beyond R_{is} surface tension forces have increasing influence, tending to make the bubble adopt a spherical shape, which may introduce dynamic forces tending to take the bubble away from the wall.

(2) As the bubble grows beyond R_{ig} (in normal gravity) gravitational body forces have increasing influence, tending to take the bubble from the wall.

Other influences are apparently involved (such as thermocapillarity) tending to affect bubble departure, or prevent it, particularly for small bubbles at high pressures.

With metallic fluids, microlayers may occur, but their effect on bubble growth will be less important.

REFERENCES

1. M. G. COOPER and A. J. P. LLOYD, The microlayer in nucleate pool boiling. *Int. J. Heat Mass Transfer* **12**, 895–913 (1969).
2. C-Y. HAN and P. GRIFFITH, The mechanism of heat transfer in nucleate pool boiling, *Int. J. Heat Mass Transfer* **8**, 887–904 (1965).
3. R. COLE and H. L. SHULMAN, Bubble growth rates at high Jakob numbers, *Int. J. Heat Mass Transfer* **9**, 1377–1390 (1966).
4. M. A. JOHNSON, J. DE LA PENA and R. B. MESLER, Bubble shapes in nucleate boiling, *J. Am. Inst. chem. Engrs* **12**, 344–348 (1966).
5. L. E. SCRIVEN, On the dynamics of phase growth, *Chem. Engng Sci.* **10**, 1–13 (1959).
6. M. G. COOPER and A. J. P. LLOYD, Transient local heat flux in nucleate boiling, 3rd *Int. Heat Transfer. Conf.*, Paper 100, Chicago (1966).
7. H. S. CARSLAW and J. C. JAEGER, *Conduction of Heat in Solids*, Oxford University Press, London (1959).
8. F. G. GUNTER, Photographic studies of surface boiling heat transfer to water with forced circulation, A.S.M.E. *Trans. Am. Soc. mech. Engrs* **73**, 115–123 (1951).
9. R. COLE, Bubble frequencies and departure diameters at subatmospheric pressures, *A.I.Ch.E. Jl* **13**, 779–783 (1967).
10. R. COLE and H. L. SHULMAN, Bubble departure diameters at subatmospheric pressures. C.E.P. Symp. Series no. 64, **62**, 6–16 (1966).
11. J. E. SHERLEY, Nucleate boiling heat transfer data for liquid hydrogen at standard and near-zero gravity. *Adv. Astronaut. Sci.* **14**, 177–195 (1964).
12. J. A. CLARK and H. MERTE, Nucleate, transition and film boiling heat transfer at zero gravity. *Adv. Astronaut. Sci.* **14**, 177–195 (1964).
13. P. GRIFFITH, Bubble growth rates in boiling. *Trans. Am. Soc. mech. Engrs* **80**, 721 (1958).
14. L. A. SKINNER and S. G. BANKOFF, Dynamics of vapour bubbles in general temperature fields *Physics Fluids* **8**, 1417–1420 (1965).
15. A. C-B. WONG, High speed microphotographic study of nucleate boiling in liquid nitrogen and liquid helium. M.Sc. Thesis, Department of Mechanical Engineering, Purdue University, Lafayette, Ind. U.S.A. (1967).

APPENDIX A1

To Develop Expression 1 of Equation (20)

The five pressure terms P_d, P_i, P_s, P_g, P_v are

$$(T_{w0} - T_{sat})\left(\frac{dp}{dT}\right)_{sat}; \rho(R\ddot{R} + \tfrac{3}{2}\dot{R}^2); \frac{2\sigma}{R}; (\rho_l - \rho_v)gR; 4\mu_l\frac{\dot{R}}{R}.$$

Using $R = C_1 t^{\frac{1}{2}}$ we have

$$\dot{R} = \tfrac{1}{2}C_1/t^{\frac{1}{2}} = C_1^2/2R \text{ and } \ddot{R} = -C_1/4t^{\frac{3}{2}} = -C_1^4/4R^3$$

hence

$$P_i = \frac{\rho C_1^4}{8R^2};\ P_v = 2\mu_l \frac{C_1^2}{R^2}.$$

Substituting

$$C_1 = \frac{2}{C_2}\frac{(T_{w0} - T_{sat})}{\phi} v_l^{\frac{1}{2}} \text{ and } (T_{w0} - T_{sat}) = \Delta T$$

and using the Clausius—Clapeyron relation to give

$$\left(\frac{dp}{dT}\right)_{sat} = \frac{h_{fg}\rho_l\rho_v}{T_{sat}(\rho_l - \rho_v)} \doteq \frac{\psi k_l}{T_{sat}v_l} (\rho_l \gg \rho_v)$$

the five pressure terms are respectively

$$\frac{\Delta T \psi k_l}{T_{sat}v_l};\ \frac{2\rho_l v_l^2}{R^2}\left(\frac{\Delta T}{C_2\phi}\right)^4;\ \frac{2\sigma}{R};$$

$$(\rho_l - \rho_v) gR;\ \frac{8\mu_l v_l}{R^2}\left(\frac{\Delta T}{C_2\phi}\right)^2$$

and the inequalities of equation (1) are respectively

$$\left\{\frac{\Delta T}{C_2\phi}\right\}^4 \gg \frac{\sigma R}{\rho_l v_l^2}$$

$$\frac{C_2\phi\psi k_l R^2}{2T_{sat}\rho_l v_l^3} \gg \left\{\frac{\Delta T}{C_2\phi}\right\}^3;\ \left\{\frac{\Delta T}{C_2\phi}\right\}^4 \gg \frac{(\rho_l - \rho_v) gR^3}{2\rho_l v_l^2}$$

$$\left\{\frac{\Delta T}{C_2\phi}\right\}^2 \gg 4$$

which reduce to the form given in equation (20) if we define

$$L_d = \left\{\frac{\rho_l v_l^3 T_{sat}}{\phi\psi k_l}\right\}^{\frac{1}{2}} \doteq \left\{\frac{\rho_l v_l^3 T_{sat}}{\psi^2 k_l}\right\}^{\frac{1}{2}} = \frac{\{\rho_l k_l v_l T_{sat}\}^{\frac{1}{2}}}{\rho_v h_{fg}}$$

$$L_s = \frac{\rho_l v_l^2}{\sigma}$$

and $$L_g = \left\{\frac{2\rho_l v_l^2}{(\rho_l - \rho_v) g}\right\}^{\frac{1}{2}}$$

APPENDIX A2

Evaporation from Microlayer and From Curved Surface

Basis—neglect of thermal boundary layer

In some theories of bubble growth the conduction of heat from the thermal boundary layer to the curved surface of the bubble is taken to be a major or sole factor causing evaporation. In their simplest form the theories regard the thermal boundary layer as being bodily displaced to surround the curved surface of the bubble (Fig. 5(a)) and then assess the rate

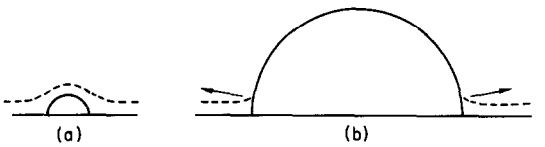

FIG. 5. (a) Bubble surrounded by thermal boundary layer. (b) Bubble growing far beyond thermal boundary layer.

of conduction of heat to the interface. Such theories may be appropriate if the bubble radius never grows much beyond θ_T (Fig. 5(a)) but they are considered inappropriate for bubbles which grow to some 10 or 100 θ_T (Fig. 5(b)). When a bubble grows greatly beyond θ_T, the liquid in the thermal boundary layer is not added to that around the curved surface. Instead it is displaced radially as shown by the arrows in Fig. 5(b). Also, the layer of hot liquid which surrounded the bubble as it grew past θ_T (Fig. 5(a)) must have been subsequently thinned out by being spread over a larger bubble surface. More rigorous analyses [13], [14] allow for these combined effects of liquid motion and thermal conduction, but they ignore the microlayer. The ultimate aim will be the further integration of those theories with microlayer evaporation, but here, as elsewhere in this paper, the analysis is largely confined to an extreme case, for simplicity. Here it is assumed that the bubble radius grows far in excess of θ_T, hence heat conduction differs little from that occurring in a liquid initially at

uniform temperature T_b. Analysis thus neglects the thermal boundary layer, but allows for evaporation from the microlayer and evaporation or condensation at the curved surface of the bubble.

A final paragraph in this appendix considers the growth of a bubble while its radius is small compared with θ_T.

Analysis

If a bubble grew at rate $R = C_1 t^{\frac{1}{2}}$ due solely to evaporation at its curved surface when immersed in liquid initially at uniform temperature T_∞, then from equations (11), (12), (19)

$$C_1 = \left\{C_2 \left(\frac{3}{\pi}\right)^{\frac{1}{2}} Pr_l^{\frac{1}{2}}\right\} \left(\frac{2}{C_2} \frac{T_\infty - T_{sat}}{\psi} v_l^{\frac{1}{2}}\right)$$

hence

$$T_\infty - T_{sat} = C_1 \frac{C_2 \psi}{2 v_l^{\frac{1}{2}}} \left\{C_2 \left(\frac{3}{\pi}\right)^{\frac{1}{2}} Pr_l^{\frac{1}{2}}\right\}^{-1}.$$

If instead the bulk temperature is T_b but the bubble radius nevertheless grows at the same rate $C_1 t^{\frac{1}{2}}$ then the fluid motion is unchanged (provided $\rho_v \ll \rho_l$) so heat flow and vapour production are changed by factor $(T_b - T_{sat})/(T_\infty - T_{sat})$ so the volume of vapour caused by evaporation at the curved surface while the bubble grows to radius R is

$$\frac{T_b - T_{sat}}{T_\infty - T_{sat}} \tfrac{2}{3}\pi R^3 \text{ on each hemisphere}$$
$$= \frac{1}{C_1} \left\{C_2 \left(\frac{3}{\pi}\right)^{\frac{1}{2}} . Pr_l^{\frac{1}{2}}\right\} \left(\frac{2}{C_2} \frac{T_b - T_{sat}}{\psi} v_l^{\frac{1}{2}}\right) \times \tfrac{2}{3}\pi R^3.$$

If a hemispherical bubble grew at rate $R = C_1 t^{\frac{1}{2}}$ due solely to microlayer evaporation with wall temperature T'_w, then from equations (9), (12)

$$C_1 = \frac{2}{C_2} \frac{T'_w - T_{sat}}{\psi} v_l^{\frac{1}{2}}$$

hence

$$T'_w - T_{sat} = C_1 \frac{C_2 \psi}{2 v_l^{\frac{1}{2}}}.$$

If instead the wall temperature is T_{w0} but the bubble radius nevertheless grows at the same rate $C_1 t^{\frac{1}{2}}$ then the fluid motion is unchanged (provided $p_v \ll \rho_l$) so the microlayer is formed with the same initial thickness δ_0. The arguments of equations (6), (7) and (8) still apply, and hence from equation (8) with $n = \frac{1}{2}$ and B substituted the volume of vapour evaporated from the microlayer is

$$V_m = \tfrac{2}{3}\pi R^3 \left\{\frac{2}{C_2} \frac{T_{w0} - T_{sat}}{\phi} \frac{v_l^{\frac{1}{2}}}{C_1}\right\}$$

and again $\phi \doteq \psi$.

For a hemispherical bubble to grow at rate $R = C_1 t^{\frac{1}{2}}$ due to the combined effects of the two mechanisms, namely evaporation at its curved surface from initial bulk temperature T_b and evaporation from the microlayer on a wall at temperature T_{w0}, we must have:

$$\tfrac{2}{3}\pi R^3 = \frac{1}{C_1} \left\{C_2 \left(\frac{3}{\pi}\right)^{\frac{1}{2}} Pr^{\frac{1}{2}}\right\} \left(\frac{2}{C_2} \frac{T_b - T_{sat}}{\psi} v_l^{\frac{1}{2}}\right) \times \tfrac{2}{3}\pi R^3 + \frac{1}{C_1} \left(\frac{2}{C_2} \frac{T_{w0} - T_{sat}}{\psi} v_l^{\frac{1}{2}}\right) . \tfrac{2}{3}\pi R^3$$

hence

$$C_1 = \left\{C_2 \left(\frac{3}{\pi}\right)^{\frac{1}{2}} Pr^{\frac{1}{2}}\right\} \left(\frac{2}{C_2} \frac{T_b - T_{sat}}{\psi} v_l^{\frac{1}{2}}\right) + \left(\frac{2}{C_2} \frac{T_{w0} - T_{sat}}{\psi} v_l^{\frac{1}{2}}\right)$$

or

$$R = \left\{C_2 \left(\frac{3}{\pi}\right)^{\frac{1}{2}} Pr^{\frac{1}{2}}\right\} \left(\frac{2}{C_2} \frac{T_b - T_{sat}}{\psi} v_l^{\frac{1}{2}}\right) t^{\frac{1}{2}} + \left(\frac{2}{C_2} \frac{T_{w0} - T_{sat}}{\psi} v_l^{\frac{1}{2}}\right) t^{\frac{1}{2}}$$

showing that the radial growth rates (not the volumetric rates) are added. If the second term in this equation is much larger than the first, then growth is largely due to evaporation of the microlayer. This yields condition 2 of equation (20).

This equation also shows that the expressions derived in this paper for saturation boiling

($T_b \doteqdot T_{sat}$) can be used for cases in which the two mechanisms are both operating, provided $[T_{w0} - T_{sat} + \{C_2(3/\pi)^{\frac{1}{2}} Pr^{\frac{1}{2}}\}(T_b - T_{sat})]$ is written in place of $(T_{w0} - T_{sat})$.

Effect of Thermal Boundary Layer on Small Bubbles

Very early in the growth of a bubble its radius is small compared with θ_T and its lifetime is short compared with θ_T^2/α_l (typically 0·1 mm, 0·1 sec for the experiments discussed here). These facts imply respectively that the bubble is deep in the thermal boundary layer, where the temperature of the liquid is nearly T_{w0} and that the presence of cooler liquid beyond is hardly felt. Hence in the limit of very small size, growth occurs under the combined influence of microlayer evaporation and growth in a superheated liquid which has effectively uniform initial temperature T_{w0}. Writing $T_b = T_{w0}$ in the above equation gives:

$$R = \left\{1 + C_2\left(\frac{3}{\pi}\right)^{\frac{1}{2}} Pr_l^{\frac{1}{2}}\right\} \frac{2}{C_2} \frac{T_{w0} - T_{sat}}{\psi} (\nu_l t)^{\frac{1}{2}}$$

$$\doteqdot (1 + 0{\cdot}78\, Pr_l^{\frac{1}{2}})\, 2{\cdot}5 \frac{Ja}{Pr_l} (\nu_l t)^{\frac{1}{2}}.$$

Few data are available for the very small sizes involved, but [15] reports experiments with liquid nitrogen boiling at a heated surface, and gives some data points for bubbles of radius less than $2\theta_T$. The initial growth rate is some 1·4 times the rate predicted for growth in a uniformly superheated liquid at T_{w0}. This is some 20% below the rate predicted by the equation above, suggesting that the two mechanisms are both operating, though not to the extent indicated by taking $T_b = T_{w0}$.

APPENDIX A3

To Develop Expression 3 of Equation (20)

Integrating equation (6) we obtain

$$\delta_0^2 - \delta^2 = \frac{2k_l}{\rho_l h_{fg}} \int_{t_g}^{t} (T_w - T_{sat})\, dt$$

and we require the condition that the integral can be adequately approximated by $(T_{w0} - T_{sat})(t - t_g)$ for $t_g < t < t_e$.

However high the conductivity of the wall, T_w must clearly fall towards T_{sat} at the end of the evaporation period. However, the approximation will be adequate provided T_w is close to T_{w0} for most of the evaporation period. Say $(T_{w0} - T_w) \ll (T_{w0} - T_{sat})$ for 95% of the evaporation period. If that is so, then equation (7) applies for most of the evaporation period. Substituting $\delta_0^2 = C_2^2 \nu_l t_g$ in that, and noting that $\delta = 0$ when $t = t_e$ we find

$$\delta = \left\{\frac{2k_l}{\rho_l h_{fg}} (T_{w0} - T_{sat})(t_e - t)\right\}^{\frac{1}{2}}.$$

Hence the heat flux can be adequately approximated during 95 per cent of the evaporation period by

$$\frac{k_l(T_{w0} - T_{sat})}{\delta} = \frac{K}{(t_e - t)^{\frac{1}{2}}}$$

where $K = \{\frac{1}{2} k_l \rho_l h_{fg} (T_{w0} - T_{sat})\}^{\frac{1}{2}}$.

But if such a heat flux is withdrawn from a semi-infinite body initially at uniform temperature, then from [7] the wall temperature falls by

$$\frac{K}{(\pi k_w \rho_w C_{pw})^{\frac{1}{2}}} \int_{\tau=0}^{\tau=t} \frac{1}{[t_e - (t - \tau)]^{\frac{1}{2}}} \frac{d\tau}{\tau^{\frac{1}{2}}}.$$

Neglecting t_g compared with t_e we apply this expression and note that the integral can be evaluated and is

$$2 \log [\{t_e/(t_e - t)\}^{\frac{1}{2}} + \{t/(t_e - t)\}^{\frac{1}{2}}]$$

which has a singularity at $t = t_e$, corresponding to the end of evaporation. Discarding the last 5 per cent of the evaporation period as discussed earlier, $t = 0{\cdot}95 t_e$ and the integral is 4·36.

The required condition can therefore be expressed as

$$\frac{K}{(\pi k_w \rho_w C_{pw})^{\frac{1}{2}}} \times 4{\cdot}36 \ll (T_{w0} - T_{sat}).$$

Substituting for K, re-arranging and writing $4{\cdot}36^2/(2\pi) = 3$ yields 3(a) of equation (20).

APPENDIX B

Failure of the Condition $P_d \gg P_i$

If $(T_{w0} - T_{sat})(\mathrm{d}p/\mathrm{d}T)_{sat}$ is not greatly in excess of $\rho_l(R\ddot{R} + \frac{3}{2}\dot{R}^2)$ with $R = C_1 t^{\frac{1}{2}}$ then the pressure p_b in the bubble differs significantly from system pressure, and the analysis given above must be discarded because it was based on taking the temperature at the top of the microlayer to be T_{sat}. An opposite extreme would be to take the temperature in the bubble to be equal to T_w, hence the pressure in the bubble would exceed the system pressure by $(T_w - T_{sat})(\mathrm{d}p/\mathrm{d}T)_{sat}$ and the growth of the bubble would be governed by

$$\rho_l(R\ddot{R} + \tfrac{3}{2}\dot{R}^2) = (T_w - T_{sat})\left(\frac{\mathrm{d}p}{\mathrm{d}T}\right)_{sat}$$

vapour being supplied by microlayer evaporation at the rate necessary to cause this growth. If further the wall temperature is nearly constant at T_{w0} then

$$R\ddot{R} + \tfrac{3}{2}\dot{R}^2 = \frac{P_d}{\rho_l}$$

which integrates to

$$\dot{R}^2 = \frac{2P_d}{3\rho_l} + \frac{\text{constant}}{R^3}.$$

The constant of integration could be determined if initial values of R, $\dot{R}$ were available. It must apparently be zero if there is to be no singularity in $\dot{R}$ for small values of R. The position is obscure and depends on the conditions of initiation of the bubble. Whatever the value of the constant, the term falls as R^{-3}. This suggests (but does not prove) that when R exceeds its initial value by an order of magnitude we can write

$$\dot{R} \doteq \left\{\frac{2}{3}\frac{T_{w0} - T_{sat}}{\rho_l}\left(\frac{\mathrm{d}p}{\mathrm{d}T}\right)_{sat}\right\}^{\frac{1}{2}}$$

until in due course the temperature drop across the microlayer becomes significant so p_b is no longer governed by T_w, and the situation is closer to that summarised in equation (1).

The toluene bubbles reported in [1] and [6] are not suited to this problem, as they soon grew past this phase (R_{di} typically less than 1 mm). Some bubbles are reported in [3] with water at 50 mm pressure for which R_{di} is 16 mm, suggesting that the theory above should apply. Due to the characteristics of the heater, a strip of zirconium 0·25 mm thick and 12·7 mm wide, some reservations arise:

(1) The thermal conductivity of zirconium is too low for the surface temperature to be regarded as constant throughout the growth period.

(2) The thickness of the strip is too low for it to be regarded as a semi infinite body for more than a few ms.

(3) The width of the strip is too small for the bubbles to grow symmetrically beyond a few mm diameter. This was observed by the authors of [3] who allowed for it for their purpose by defining an equivalent diameter D_s assuming the bubble to be a prolate ellipsoid. If their method of determining D_s is applied to a hemispherical bubble, it will yield

$$D_s = R\sqrt[3]{2}.$$

By confining attention to the first 5 ms of bubble growth, reservations 1 and 2 above are largely avoided. Further, the bubble is then small and unlikely to be distorted by the finite width of the strip, so it is assumed that the bubble is nearly hemispherical and the bubble diameter D_s quoted in [3] is in fact about $R\sqrt[3]{2}$. In that case the prediction is that the bubble will at first grow linearly with

$$\frac{\mathrm{d}}{\mathrm{d}t}(D_s) = \sqrt[3]{2}\left\{\frac{2}{3}\frac{T_{w0} - T_{sat}}{\rho_l}\left(\frac{\mathrm{d}p}{\mathrm{d}T}\right)_{sat}\right\}^{\frac{1}{2}} = 2{\cdot}8 \text{ m/s}.$$

Comparison with the three such bubbles reported in [3] relies on some 5 or 7 frames of each cine film. As far as can be judged from

these, the bubbles do grow linearly for the first 5 or 7 ms, at rates in the range:

$$1{\cdot}8 < \frac{\mathrm{d}}{\mathrm{d}t}(D_s) < 2{\cdot}6 \text{ m/s}.$$

In view of the many extreme assumptions underlying the theory, this agreement with one set of three experimental results is not conclusive, and may be fortuitous, but it seems interesting.

Résumé—On présente une théorie afin de détermine la vitesse de croissanc d'une bulle de vapeur grossissant à partir d'une paroi chauffée dans un liquide qui est voisin de la température de saturation. La théorie des hypothèses approchées obtenues à partir des expériences dans lesquelles on *o* observà que des couches liquides minces (microcouches) se trouvaient sous de telles bulles, et dans lesquelles l'évaporation des microcouches contribuait de façon importante à la croissance des bulles. Pour simplifier l'analyse, on l'a fondée sur des hypothèses représentatives de situations plus extrêmes qui n'ont pas été explorées auparavant. Les prévisions de la théorie ont une certaine relation (±25 pour cent) avec les résultats des expériences pour divers fluides sous des conditions telles que les hypothèses soient valables de façon approchée. Ces prévisions, en même temps que des limitations associées aux gammes de validité des hypothèses, indiquent les conditions sous lesquelles on peut s'attendre a ce que les microcouches aient des effets importants sur la croissance des bulles. Elles ont aussi des conséquences sur la taille de départ des bulles, pour une gravité standard et réduite. On a discuté les cas de l'eau, des liquides organiques, des fluides-métalliques et cryogéniques.

La théorie est étndue pour y inclure l'ébullition avec une température moyenne du liquide différant de façon importante de la température de saturation.

Zusammenfassung—Zur Bestimmung der Wachstumsrate einer Dampfblase, die an einer beheizten Wand in einer Flüssigkeit mit annähernd Sättigungstemperatur entsteht, wird eine Theorie aufgestellt. Die Theorie stützt sich auf Näherungsannahmen, die aus Versuchen stammen, bei denen das Auftreten dünner Flüssigkeitsschichten (Mikroschichten) unter solchen Blasen beobachtet wurde und bei denen die Verdampfung der Mikroschichten massgeblich zum Wachstum der Blasen beiträgt. Zur Vereinfachung basiert die Betrachtung auf Annahmen, die für extremere Zustände typisch sind bei denen die Mikroschicht vorherrscht, Extreme die bisher noch nicht erforscht worden sind. Die Voraussagen lassen sich mit einiger Berechtigung (±25 Prozent) auf die experimentellen Ergebnisse für verschiedene Flüssigkeite bei welchen die Annahmen annähernd gültig sind, anwenden. Diese Voraussagen zusammen mit den aufgeführten Einschränkungen des Gültigkeitsbereiches der Annahmen weisen auf die Bedingungen hind unter denen erwartet werden kann, dass die Mikroschichten einen bedeutenden Einfluss auf das Blasenwachstum haben. Es ergeben sich daraus auch Folgerungen für die Blasenabreissgrösse bei normalem und reduziertem Schwerefeld. Es werden Wasser, organische Flüssigkeiten, Kältemittel und flüssige Metalle untersucht.

Die Theorie ist erweitert worden, um das Sieden bei Flüssigkeitstemperaturen zu erfassen, die sich wesentlich von der Sättigungstemperatur unterscheiden.

Аннотация—Предложена теория определения скорости роста пузырька пара на нагреваемой стенке в жидкости, температура которой близка к температуре насыщения. Она основывается на приближенных допущениях, полученных экспериментальным путем, когда под такими пузырьками наблюдались тонкие слои жидкости (микрослои) и когда испарение микрослоев значительно способствовало росту пузырьков. Для упрощения анализа брались допущения, характерные для экстремальных ситуаций, когда доминирует микрослой. Эти случаи ранее исследованы не были. Аналитические расчеты дают некоторое совпадение (±25 %) с результатами экспериментов с различными жидкостями, для которых эти допущения являются приближенно справедливыми. Аналитические расчеты и связанные с ними ограничения о диапазонах справедливости допущений показывают, при каких условиях микрослои могут оказывать значительное влияние на рост пузырей. Они также оказывают влияние на размер пузырька во время отрыва при обычных и пониженных значениях силы тяжести. Рассматривались вода, органические и криогенные жидкости, а также жидкие металлы.

Теория распространяется на случай кипения, когда объемная температура жидкости значительно отличается от температуры насыщения.